Inorg. Chem. **2005**, *44*, 9743–9751

X-ray Diffraction and EXAFS Studies of Hydroxo–Cu(II) Complexes Based on a Calix[6]arene-N_3 Ligand: Evidence for a Mononuclear–Dinuclear Equilibrium Controlled by Supramolecular Features

Guillaume Izzet,[†] Yves M. Frapart,[†] Thierry Prangé,[‡] Karine Provost,[§] Alain Michalowicz,[§] and Olivia Reinaud*,[†]

Laboratoire de Chimie et Biochimie Pharmacologiques et Toxicologiques, UMR CNRS 8601, Université René Descartes, 45 rue des Saints-Pères, 75270 Paris Cedex 06, France, Laboratoire de Cristallographie et RMN Biologiques, UMR CNRS 8015, Université René Descartes, 4 avenue de l'Observatoire, 75270 Paris Cedex 06, France, and Groupe de Physique des Milieux Denses, Université Paris XII-Val de Marne, 61 Avenue du Général De Gaulle, 94010 Créteil Cedex, France

Received July 8, 2005

The formation of hydroxo complexes based on a calix[6]trisimidazole ligand is described. Deprotonation of the mononuclear Cu(II)–aqua complex gives rise to a dinuclear bis(μ-hydroxo) complex that has been characterized by X-ray diffraction analysis. Spectroscopic studies (EPR and UV–vis), conducted in dichloromethane solutions in the presence of various coordinating cosolvents (DMF, EtOH, or RCN) or with acetamide, revealed the coexistence of a mononuclear hydroxo species. The latter could be trapped by acetic acid to provide an acetato–Cu(II) complex that presents close spectroscopic features. An EXAFS study first conducted on the hydroxo–Cu(II) complex led to an excellent fit for the dinuclear core. It then allowed for the characterization of the mononuclear acetato complex with an acetamide guest included in the calixarene cavity. Hence, this study illustrates the flexibility of calixarene-based ligands and the role of the second coordination sphere in the stabilization of acidic or basic Cu(II) complexes.

Introduction

Metal centers with hydroxo ligands are important functional units in metalloproteins. They are proposed to be active species in a variety of enzymes, including zinc and nickel hydrolytic enzymes, iron and cobalt nitrile hydratase, iron-containing lipoxygenases, and acid phosphatase.[1,2] They are also proposed as intermediates in the oxygen-evolving complexes in copper monooxygenases and oxidases.[3] Various nuclearities can be found in these natural systems, mainly mono-, di-, or trinuclear. Modeling the natural core present in the active site is a general strategy for getting better insight into the complexes' reactivities. Dinuclear complexes presenting a bis(μ-hydroxo) core have been widely described, as they behave as thermodynamic sinks when ligands of medium steric encumbrance dress the metal ion. This is because of the bridging properties of the hydroxo ligand. In the specific case of copper, this has been largely illustrated.[4,5] Mononuclear hydroxocopper complexes are difficult to stabilize, and only a few examples of such species have been reported.[6] Indeed, their stabilization requires the conception of ligands that induce a strong steric hindrance around the

* To whom correspondence should be addressed. E-mail: Olivia.Reinaud@univ-paris5.fr.

[†] Laboratoire de Chimie et Biochimie Pharmacologiques et Toxicologiques, Université René Descartes.

[‡] Laboratoire de Cristallographie et RMN Biologiques, Université René Descartes.

[§] Université Paris XII-Val de Marne.

(1) Reviews of bioinorganic enzymology: *Chem. Rev.* **1996**, *96*, 2237−3042.

(2) MacBeth, C. E.; Hammes, B. S.; Young, V. G., Jr.; Borovik, A. S. *Inorg. Chem.* **2001**, *40*, 4733−4741.

(3) (a) Kaim, W.; Rall, J. *Angew. Chem., Int. Ed.* **1996**, *35*, 43−60. (b) Klinman, J. P. *Chem. Rev.* **1996**, *96*, 2541−2562. (c) Solomon, E. I.; Chen, P.; Metz, M.; Lee, S.-K.; Palmer, A. E. *Angew. Chem., Int. Ed.* **2001**, *40*, 4570−4590.

(4) For reviews, see: (a) Hatcher, L. Q.; Karlin, K. D. *J. Biol. Inorg. Chem.* **2004**, *9*, 669−683. (b) Lewis, E. A.; Tolman, W. B. *Chem. Rev.* **2004**, *104*, 1047−1076. (c) Mirica, L. M.; Ottenwaelder, X.; Stack, T. D. P. *Chem. Rev.* **2004**, *104*, 1013−1045.

10.1021/ic0511322 CCC: $30.25
Published on Web 11/23/2005

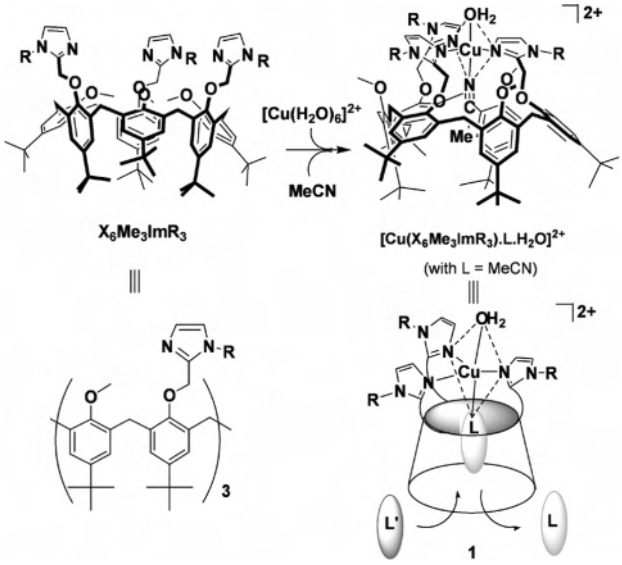

Figure 1. $X_6Me_3ImR_3$ and the corresponding Cu(II) dicationic complexes.

metal center in order to prevent the dimerization of the complex. The introduction of hydrogen bonding sites (such as an amide) on the ligand has also been shown to be a good strategy for the stabilization of such basic species. Hence, the second coordination sphere of these hydroxo complexes seems to play a major role in their structurations and reactivities.

We have developed a supramolecular system that mimics not only the polyhistidine core that binds a monocopper ion but also the hydrophobic pocket that controls the second coordination sphere of the metal as well as its binding to an exogenous molecule. The model is based on a calix[6]arene functionalized with three nitrogenous moieties ($X_6Me_3N_3$) that have been covalently linked to the narrow rim of the calixarene. With a tris(pyridine) coordinating core,[7] the system best stabilizes the copper(I) state, whereas a tris(imidazole)-based ligand ($X_6Me_3ImR_3$, see Figure 1) yields very stable Cu(II) complexes.[8] The synthesis and characterization of the corresponding dicationic complexes $[Cu(X_6Me_3ImR_3)(L)(H_2O)]^{2+}$ have been previously described. Two of them have been characterized by X-ray crystallography. Both revealed a five-coordinate cupric center within a distorted square-based pyramidal (SBP) geometry in a $N_3L(H_2O)$ environment. In this system, a small organic guest ligand L selectively coordinates Cu(II) in the heart of the calixarene cavity, whereas a water molecule caps the edifice from the outside. The guest molecule L can be selectively substituted by other small organic ligands L′ (Figure 1).

In this paper, we describe the synthesis and solid and solution structures of the corresponding Cu^{II}−hydroxo complexes. These novel species mainly exist as dinuclear complexes. However, in solution, an equilibrium between a mononuclear and a dinuclear hydroxo complex has been evidenced.

Experimental Section

All solvents and reagents were obtained commercially. THF was distilled from sodium/benzophenone under argon, and acetonitrile was distilled from calcium hydride under argon. IR spectra were recorded with a Perkin-Elmer spectrum one spectrometer. Elemental analyses were performed at the Institut des Substances Naturelles, Gif sur Yvette, France. The UV−vis spectra were recorded with a Jasco V-570 spectrophotometer. The EPR spectra were recorded at 90 K, using a Bruker ELEXSYS 500 spectrometer fitted with a SHQ001 cavity. The following parameters were chosen: microwave power of 10 mW, modulation amplitude of 0.6 mT, modulation frequency of 100 kHz, and microwave frequency of about 9.44581 GHz (X-band).

Caution: Although we have not encountered any problems, it is noted that perchlorate salts of metal complexes with organic ligands are potentially explosive and should be handled only in small quantities with appropriate precautions.

Synthesis of 2. Under argon, a dry THF solution (3 mL) containing $Cu(ClO_4)_2(H_2O)_6$ (32.8 mg, 88.5 μmol) was added to the solid ligand $X_6Me_3Imme_3$ (115 mg, 88.5 μmol). The resulting cobalt blue-green solution was stirred for 30 min. A stoichiometric amount of NBu_4OH in a 9:1 (v/v) THF/MeOH mixture (885 μL of 0.1 M solution, 88.5 μmol) was subsequently added to the reaction mixture, which was stirred for 30 min. After separation of a very small precipitate by centrifugation, we removed the solvents under vacuum. The residue was redissolved in methanol to give a green homogeneous solution out of which a precipitate appeared after a few minutes. The solid compound was collected by centrifugation, and was washed twice with methanol to yield **2** as a blue solid (80 mg, 60%).

2 could also be directly obtained from the reaction of complex **1** in THF with NBu_4OH following the exact same procedure as described above.

IR: (KBr) ν 2960, 1628, 1481, 1415, 1394, 1363, 1290, 1242, 1202, 1108, 1007, 874, 623 cm^{-1}; (in CH_2Cl_2) ν_{OH} 3555 cm^{-1}. Anal. Calcd for $[Cu(C_{84}H_{108}N_6O_6)(OH)]_2(ClO_4)_2(H_2O)_4$: C, 66.65; H, 7.52; N, 5.55. Found: C, 66.20; H, 7.36; N, 5.55.

X-ray Diffraction Study. Diffraction data were recorded at the synchrotron DCI facility in Orsay, France. As the crystals were unstable when exposed to air, they were fished out of their mother

(5) (a) Kitajima, N.; Koda, T.; Hashimoto, S.; Kitagawa, T.; Moro-oka, Y. *J. Am. Chem. Soc.* **1991**, *113*, 5664−5671. (b) Kitajima, N.; Fujisawa, K.; Fujimoto, C.; Moro-oka, Y.; Hashimoto, S.; Kitagawa, T.; Toriumi, K.; Tatsumi, K.; Nakamura, A. *J. Am. Chem. Soc.* **1992**, *114*, 1277−1291. (c) Spencer, D. J. E.; Reynolds, A. M.; Holland, P. L.; Jazdzewski, B. A.; Duboc-Toia, C.; Le Pape, L.; Yokota, S.; Tachi, Y.; Itoh, S.; Tolman, W. B. *Inorg. Chem.* **2002**, *41*, 6307−6321. (d) Lam, B. M. T.; Halfen, J. A.; Young, V. G., Jr.; Hagadorn, J. R.; Holland, P. L.; Lledós, A.; Cucurull-Sánchez, L.; Novoa, J. J.; Alvarez, S.; Tolman, W. B. *Inorg. Chem.* **2000**, *39*, 4059−4072. (e) Mukherjee, J.; Mukherjee, R. *Inorg. Chim. Acta* **2002**, *337*, 429−438. (f) Zhang, C. X.; Liang, H.-C.; Kim, E.-I.; Shearer, J.; Helton, M. E.; Kim, E.; Kaderli, S.; Incarvito, C. D.; Zuberbühler, A. D.; Rheingold, A. L.; Karlin, K. D. *J. Am. Chem. Soc.* **2003**, *125*, 634−635.

(6) (a) Lee, S. C.; Holm, R. H. *J. Am. Chem. Soc.* **1993**, *115*, 11789−11798. (b) Berreau, L. M.; Mahapatra, S.; Halphen, J. A.; Young, V. G., Jr.; Tolman, W. B. *Inorg. Chem.* **1996**, *35*, 6339−6342. (c) Harata, M.; Hasegawa, K.; Jitsukawa, K.; Masuda, H.; Einaga, H. *Bull. Chem. Soc. Jpn.* **1998**, *71*, 1031−1038. (d) Fujisawa, K.; Kobayashi, T.; Fujita, K.; Kitajima, N.; Moro-oka, Y.; Miyashita, Y.; Yamada, Y.; Okamoto, K. *Bull. Chem. Soc. Jpn.* **2000**, *73*, 1797−1804. (e) Tubbs, K. J.; Fuller, A. L.; Bennett, B.; Arif, A. M.; Berreau, L. M. *Inorg. Chem.* **2003**, *42*, 4790−4791.

(7) (a) Blanchard, S.; Le Clainche, L.; Rager, M.-N.; Chansou, B.; Tuchagues, J.-P.; Duprat, A. F.; Le Mest, Y.; Reinaud, O. *Angew. Chem., Int. Ed.* **1998**, *37*, 2732−2735. (b) Rondelez, Y.; Rager, M.-N.; Duprat, A.; Reinaud, O. *J. Am. Chem. Soc.* **2002**, *124*, 1334−1340.

(8) (a) Le Clainche, L.; Giorgi, M.; Reinaud, O. *Inorg. Chem.* **2000**, *39*, 3436−3437. (b) Le Clainche, L.; Rondelez, Y.; Sénèque, O.; Blanchard, S.; Campion, M.; Giorgi, M.; Duprat, A. F.; Le Mest, Y.; Reinaud, O. *C. R. Acad. Sci., Ser. IIc: Chim.* **2000**, *3*, 811−819.

Table 1. Data Processing and Refinement Statistics for **2a**

formula (asymmetric unit)	$C_{168}H_{216}Cu_2N_{12}O_{14}$
overall formula (including solvents and counterions)	$C_{174.58}H_{230.95}Cl_{8.05}Cu_2N_{12}O_{22.89}$
space group	triclinic; $P1$ ($Z = 1$)
a (Å)	15.279(4)
b (Å)	16.130(4)
c (Å)	22.828(4)
α (deg)	69.67(7)
β (deg)	80.58(8)
γ (deg)	64.63(8)
T (K)	193
V (Å^3)	4766
total no. of reflns measured	22741
resolution limits (Å) (last shell)	11.7−1.09 (1.13−1.09)
completeness (%)	91.4
R_{sym} (%) overall	7.5
R_{sym} (%) last resolution shell	11.9
no. of independent reflns	8041
no. of obs reflns(*)	6448
R (observed F data)	0.0762
R (all F data)	0.0784
R (observed F^2 data)	0.2194
R (all F^2 data)	0.2229
no. of refined atoms	234
no. of params/no. of restraints	1810/2343
min/max (e$^-$) in last electron density	−0.38/+0.59
CCDC deposit number	198692

liquor using a cryoloop, rapidly mounted on the goniometer head of the diffraction device (MAR Research 345 Image Plate), and frozen under a cold nitrogen stream. Data sets consist of 100 frames, 3° rotation each (exposure time: 6 s). Frames were processed using the *DENZO*/*HKL* package.[9]

The structure was solved using the *SHELXD*[10] program. Refinements were processed using *SHELXL* and then *SHELXH*.[11] programs. Although initially solved in the centrosymmetric $P\bar{1}$ space group with one calix[6]arene moiety and one copper ion in the asymmetric unit, refinements converged only in the noncentrosymmetric space group $P1$ using the full dinuclear complex because of a particular noncentrosymmetric distribution of the solvent. Five dichloromethanes, two perchlorate counterions, and one molecule of ether were included. Most of the agitated (disordered) *t*Bu groups of the calixarenes were kept isotropic. Constraints on 1,2 and 1,3 bond distances were applied, as well as flat ring constraints for the benzene and imidazole rings. Hydrogen atoms were introduced in calculated positions, with their isotropic thermal factor riding on that of the bonded atom (Table 1).

EPR Simulations. The EPR spectra were simulated using the *XSOPHE* computer simulation suite (Bruker). We first simulated the copper signature of each spectrum. This signal was then subtracted from the original spectrum in order to obtain the hyperfine signature at $g = 2$. This subtracted spectrum was then simulated alone. A final refinment was processed using the following Hamiltonian (eq 1) with the parameters given in Table 2:

$$H = (g)\beta S + S|A|I_{Cu} + 2S|A|I_N \quad (1)$$

EXAFS Studies. The EXAFS spectra of complexes **2** and **3** were recorded at the Laboratoire pour l'Utilization du Rayonnement Electromagnétique, Paris-Sud University (LURE), on the EXAFS13

Table 2. EPR Data of Compound **2** in Various Solvent Systems

solvent	g	A_{Cu} ($\times 10^{-4}$ cm^{-1})	A_N ($\times 10^{-4}$ cm^{-1})
THF	2.019	0	14.70
	2.079	0	15.65
	2.265	168	0
THF/DMSO 1:1	2.019	0	14.70
	2.079	0	15.65
	2.285	160	0
THF/MeCN 1:1	2.019	0	14.70
	2.079	0	15.65
	2.270	176	0
THF saturated with acetamide	2.056	0	14.70
	2.073	0	15.65
	2.280	163	0

line of the storage ring DCI. The EXAFS data analyses were performed with the EXAFS pour le Mac package, including *EXAFS-98* and *RoundMidnight* programs,[25] on an Apple Macintosh personal computer. These standard EXAFS analyses[12] include linear pre-edge background removal, polynomial and cubic spline atomic absorption calculation, McMaster's table EXAFS spectra normalization,[13] and reduction of the absorption data $\mu(E)$ to the EXAFS curve $\chi(k)$, with k defined in eq 2

$$k = \sqrt{\frac{2m_e}{\hbar^2}(E - E_0)} \quad (2)$$

where E_0 is the energy threshold, taken at the inflection point of the copper absorption (8990 ± 1 eV). Radial distribution functions $F(R)$ were calculated by Fourier transformations of $k^3w(k)\chi(k)$ in the range 2.20−12.00 Å^{-1}; $w(k)$ is a Kaiser−Bessel apodization window with a smoothness coefficient $\tau = 3$. The noise was removed by Fourier filtering. First-shell filtered spectra were fitted in order to get first-neighbor distances and error bars. The models were built using the molecular modeling software ChemBats3D interfaced to the ab initio EXAFS program *FEFF7*[24] via the *CRYSTALFF*[26a] utility. The fits of the first-shell distances were done by comparing the experimental spectra to the EXAFS standard formula (eq 3).

$$k\chi(k) = -S_0{}^2 \sum_i \frac{N_i}{R_i^2}|f_i(k,R_i)|e^{-2\sigma_i^2k^2}e^{[-2R_i/\lambda(k)]}\sin[2kR_i + 2\delta_1(k) + \psi_i(k,R_i)] \quad (3)$$

The sum is done on the single scattering paths. $S_0{}^2$ is the inelastic reduction factor. N_i is the number of equivalent scattering paths with an effective distance R_i. $\lambda(k)$ is the mean-free path of the photoelectron. σ_i is the Debye−Waller coefficient, characteristic of the width of the distance distribution for path i. $\delta_1(k)$ is the central-atom phase shift, and×f7 $f_i(k)$×f7 and $\psi_i(k)$ are the amplitude and phase of the atomic scattering factors, respectively, calculated

(9) Otwinowsky, Z.; Minor, W. *Methods Enzymol.* **1997**, *276*, 307−326.
(10) Schneider, T. R.; Sheldrick, G. M. *Acta Crystallogr.* **2002**, *D58*, 1772−1779.
(11) Sheldrick, G. M. *SHELXL97 Program for the Refinement of Crystal Structures*; University of Göttingen: Göttingen, Germany, 1997.
(12) (a) Teo, B. K. *Inorganic Chemistry Concepts, EXAFS: Basic Principles and Data Analysis*; Springer-Verlag: Berlin, 1986; Vol. 9. (b) Königsberger, D. C. *X-ray Absorption Principles, Applications, Techniques of EXAFS, SEXAFS and XANES*; Wiley: New York, 1988. (c) Lytle, F. W.; Sayers, D. E.; Stern, E. A. *Physica B* **1989**, *158*, 701−722. (d) IXS Standards and Criteria Subcommittee; *Error Reporting Recommendations*; International XAFS Society: Chicago, IL, 2000; http://ixs.iit.edu/subcommittee_reports/sc/.
(13) (a) MacMaster, W. H.; Kerr Del Grande, N.; Mallet, J. H.; Hubbell, J. H. *Compilation of X-ray Cross Sections*; National Technical Information Services: Springfield, VA, 1969. (b) Bandyopadhyay, P. *Mucal*; http:// ixs.csrri.iit.edu/database/programs/mcmaster.html.

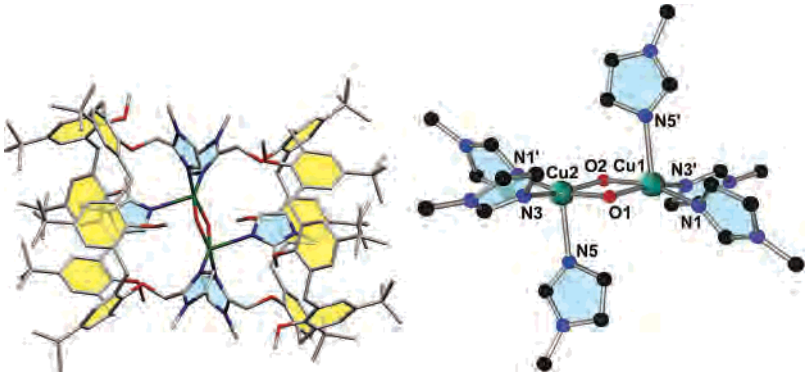

Figure 2. Crystal structure of $[Cu(X_6Me_3Imme_3)(OH)]_2(ClO_4)_2$ (**2a**) (left). Enlarged view of the dinuclear copper core (right). Hydrogen atoms, perchlorate counterions, and solvent of crystallization have been omitted for clarity.

by the code FEFF on the structural models. Because the theoretical phase shifts were utilized, it is necessary to fit the energy threshold E_0 by adding an extra fitting parameter, ΔE_0.

Once the first-shell distances were determined as described above, a complete model was constructed with ChemBats3D. The theoretical spectrum of the model was then calculated ab initio using FEFF7. This model is refined by the optimization of two parameters for each scattering group, an effective Debye−Waller factor σ_i and an effective distance shift ΔR, which are defined in the EXAFS modeling sections. The corresponding simplified EXAFS formula is as follows

$$k\chi(k) = \sum_i N_i |a_i(k)| e^{-2\sigma_i^2 k^2} \sin[2k\Delta R_i + \Phi_i(k,R_i)] \quad (4)$$

where $a_i(k)$ and $\Phi_i(k)$ are the effective amplitudes and phases of each scattering group calculated by FEFF7, respectively. It must be noted that each term of eq 3 is based on eq 2, where the sum is restricted to the most important single and multiple scattering signals of the group. If the molecular model is correct, the refined distance shifts should stand near 0 within the error bars.

The goodness of fit is given by the minimum value of the statistical $\Delta\chi^2$ and of the reduced $\Delta\chi_\nu^2$ (quality factor), where N_{ind} is the number of independent points, N_{pt} the total number of experimental points, ϵ_i^2 the experimental error, and $\nu = N_{ind} - N_{par}$ the degrees of freedom for N_{par} fitted parameters (eq 5)

$$\Delta\chi^2_{stat} = \frac{N_{ind}}{N_{pt}} \sum_i \frac{[k\chi_{th}(i) - k\chi_{exp}(i)]^2}{\epsilon_i^2}$$

$$\Delta\chi^2_\nu = \frac{\Delta\chi^2_{stat}}{\nu} \quad (5)$$

and the error bars are estimated in the standard manner, using the statistical $\Delta\chi^2$.[12c,d] Experimental error bars were estimated by the method proposed by Vlaic.[14] For this statistical evaluation, the noisiest EXAFS spectrum was chosen. The choice between equivalent models was guided by an EXAFS version of the statistical F-test.

Synthesis and Spectroscopic Characterizations

Cupric complex $[Cu(X_6Me_3Imme_3)(OH_2)_2](ClO_4)_2$ **1** (R = Me, Figure 1) was reacted with 1 equiv of NBu_4OH in a 99:1 THF/MeOH mixture to give new compound **2** that was isolated as a solid. Its elementary analysis was in agreement with a 1:1:1 copper:ligand:perchlorate ratio, and the presence of 1 equiv of perchlorate per calixarene unit was confirmed by infrared spectroscopy.

Table 3. Selected Interatomic Distances (Å) and Angles (deg) for Complex **2a**

Cu1−N1	1.980(9)	Cu2−N1′	2.004(9)
Cu1−N3′	2.025(9)	Cu2−N3	2.017(9)
Cu1−N5′	2.444(10)	Cu2−N5	2.472(10)
Cu1−O1	1.931(8)	Cu2−O1	1.961(8)
Cu1−O2	1.936(8)	Cu2−O2	1.956(8)
Cu1···Cu2	2.992(5)	O1···O2	2.490(6)
O1−Cu1−O2	80.2(4)	O1−Cu2−O2	78.9(4)
O1−Cu1−N1	91.7(5)	O1−Cu2−N1′	164.6(4)
O1−Cu1−N3′	161.7(5)	O1−Cu2−N3	90.1(5)
O1−Cu1−N5′	88.5(5)	O1−Cu2−N5	93.8(4)
O2−Cu1−N1	162.6(5)	O2−Cu2−N1′	93.8(5)
O2−Cu1−N3′	88.6(5)	O2−Cu2−N3	163.5(5)
O2−Cu1−N5′	92.8(4)	O2−Cu2−N5	89.3(4)
N1−Cu1−N3′	95.0(5)	N1′−Cu2−N3	93.8(5)
N1−Cu1−N5′	102.4(4)	N1′-Cu2−N5	99.7(4)
N3′−Cu1−N5′	106.5(5)	N3−Cu2−N5	103.8(4)
Cu1−O1−Cu2	100.5(5)	Cu1−O2−Cu2	100.5(5)

X-ray Diffraction Analysis. Single crystals were obtained by slow diffusion of ether into a solution of **2** in dichloromethane in the presence of a small quantity of methanol. The molecular structure (Figure 2) shows a binuclear bis(μ-hydroxo) complex presenting two Cu(II) ions in square-based pyramidal (SBP) geometry ($\tau_1 = 0.02$, $\tau_2 = 0.01$).[15] The Cu_2O_2 core is located between two calix[6]arene-based ligands that are stacked head to head in a cone conformation. The base of each pyramid is constituted by two imidazole groups belonging to two different calixarenes and by two bridging hydroxyls. The Cu−O bond lengths (1.93−1.96 Å) as well as the Cu···Cu and O···O distances [d(Cu1···Cu2) = 2.99 Å, d(O1···O2) = 2.49 Å] are similar to those reported for other bis(μ-hydroxo)dicopper(II) complexes (Table 3).[4] The apical position is occupied by the third imidazole self-included in the calixarene cavity thanks to a folding of the corresponding arm. The *N*-methyl substituent selectively points toward one calixarene aromatic ring at a relatively short distance [d(C···Ar) = 3.9 Å], which denotes stabilizing CH−π interactions. A similar self-inclusion process was

(14) Vlaic, G.; Andreatta, D.; Cepparo, A.; Colavita, P. E.; Fonda, E.; Michalowicz, A. *J. Synchrotron Radiat.* **1999**, *6*, 225−227.

(15) Addison, A. W.; Rao, T. N.; Reedijk, J.; Van Rijn, J.; Verschoor, G. C. *J. Chem. Soc., Dalton Trans.* **1984**, 1349−1356.

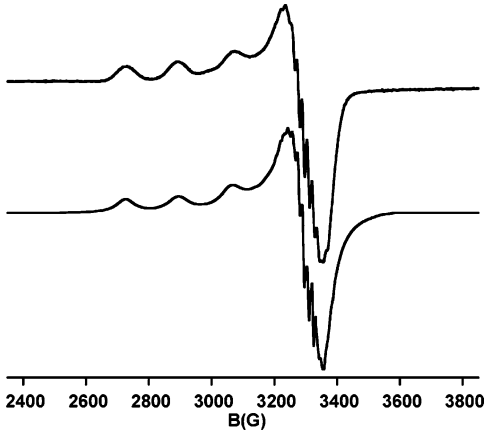

Figure 3. Experimental (top, X-band, 100 K) and simulated EPR spectra of **2** in THF. ($g_z = 2.265$, $A_{//}^{Cu} = 168.0 \times 10^{-4}$ cm^{-1}, $g_y = 2.079$, $A_y^N = 15.6 \times 10^{-4}$ cm^{-1}, $g_x = 2.019$, $A_x^N = 14.7 \times 10^{-4}$ cm^{-1}).

previously observed in the X-ray structure of the tetranuclear complex $[Cu_4(X_6Me_3Imme_3)_2(OH)_4(Cl)_2](PF_6)_2$.[16]

Evidence for a Mononuclear−Dinuclear Equilibrium. The UV−vis spectrum of **2** in dichloromethane presented a weak absorption at 600 nm ($\epsilon = 80$ M^{-1} cm^{-1}) that corresponds to a d−d transition for a Cu(II) ion in tetragonal geometry.[17] It also showed an intense absorption at 332 nm ($\epsilon = 2100$ M^{-1} cm^{-1}) consistent with a charge-transfer transition OH → Cu^{II}.[5,6] Its infrared spectrum in the same solvent showed an absorption at 3555 cm^{-1}, in agreement with a OH vibration.[5,6]

The EPR spectrum of **2** in the solid state was almost silent, as expected for such dinuclear μ-OH bridged Cu(II) complexes that are known to undergo anti-ferromagnetic coupling. However, when **2** was dissolved in THF, its EPR response increased from ca. 5 to 10% of what is expected for a mononuclear complex.[18] This attests to the presence of a new minor paramagnetic compound **2b**. The best simulation of the spectrum yielded *g* values suggesting that the metal center sits in a slightly distorted SBP geometry with two nitrogen donors in the base of the pyramid (Figure 3). Upon dilution of the solution or addition of various small coordinating molecules such as MeCN, DMSO, or DMF, the residual EPR signals slightly increased in intensity with the parameters varying as a function of the nature of the exogenous ligand (Table 2).

All these observations suggest the existence of an equilibrium between a minor mononuclear species (**2b**) that is EPR active and a major, EPR silent, dinuclear complex **2a** that corresponds to the species characterized by X-ray diffraction (Scheme 1). The equilibrium can be slightly displaced by either dilution or introduction of a small exogenous ligand that likely plays the role of a guest ligand

Scheme 1. Equilibrium between Dinuclear and Mononuclear Hydroxo Complexes **2a** and **2b**, and Subsequent Trapping of the Mononuclear Species as the Acetato Complex **3** with L = $MeCONH_2$[a]

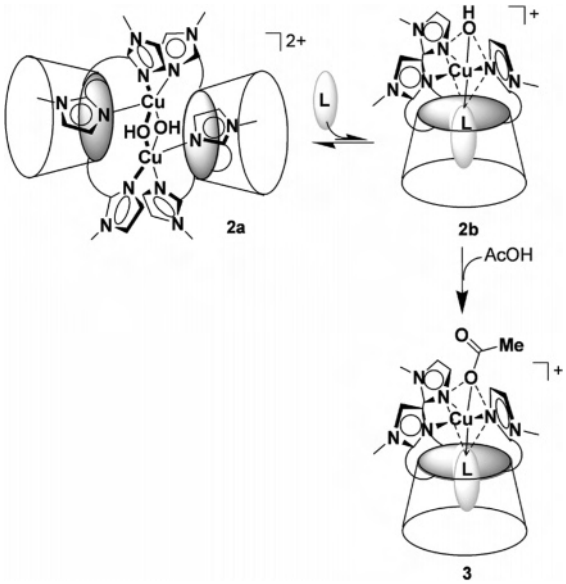

[a] The square base of the pyramid is shown with dashed lines.

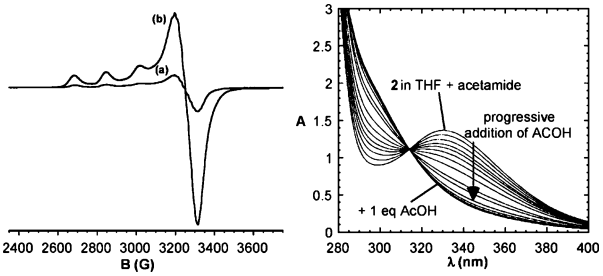

Figure 4. EPR spectra (X-band, 100 K) of (a) **2** in THF in the presence of acetamide (4 equiv) and (b) after addition of 1 equiv of acetic acid per copper ion, yielding **3** (left). Evolution of the UV−vis absorption of a THF solution containing compound **2** (5×10^{-4} M) and acetamide (30 equiv vs copper) upon the addition of aliquots of acetic acid (0 to 1 equiv) (right).

in the supramolecular system, as evidenced for the parent dicationic complex. Indeed, according to Peisach and Blumberg,[19] the EPR parameters of species **2b** are in full agreement with SBP complexes presenting either a N_2O_2 or a N_3O square base. Hence, we propose species **2b** to be a five-coordinate mononuclear complex with two imidazoles, one hydroxide, and a guest ligand in the base of the pyramid, and a third imidazole group as the apical ligand.[20]

(16) Sénèque, O.; Campion, M.; Douziech, B.; Giorgi, M.; Rivière, E.; Journaux, Y.; Le Mest, Y.; Reinaud, O. *Eur. J. Inorg. Chem.* **2002**, 2007−2014.

(17) Hathaway, B. J.; Billing, D. E. *Coord. Chem. Rev.* **1970**, *5*, 143−207.

(18) The EPR double integrations allowed us to evaluate the quantity of mononuclear Cu(II) (spin 1/2) by comparing it with the EPR response in the same solvent and same temperature of the parent dicationic complex (**1**, same quantity in the same volume).

(19) Peisach, J.; Blumberg, W. E. *Arch. Biochem. Biophys.* **1974**, *165*, 691−708.

(20) The geometry of the mononuclear complex, as proposed in Scheme 1, is quite similar to that obtained with Cu(II) and a calixarene-based ligand presenting a phenolate group covalently bound to one of the nitrogenous arm: Sénèque, O.; Campion, M.; Douziech, B.; Giorgi, M.; Le Mest, Y.; Reinaud, O. *J. Chem. Soc., Dalton Trans.* **2003**, 4216−4218. Simple modeling (Dreiding or ChemBats3D) indicates overcongestion around the metal center because of steric interactions with the calixarene core and the methoxy substituents for a hypothetical structure involving simultaneously (i) endo binding of an imidazole and (ii) exo binding of the two other imidazolse + OH + guest. In the dinuclear structure, the Cu(II) ions are bound in the exo position to two imidazole arms belonging to two different calixarenes, which allows for relative steric decongestion. Such a steric constraint due to the macrocycle actually leads to the formation of tri- and tetranuclear species in the presence of extra copper and anions. See refs 16 and 27.

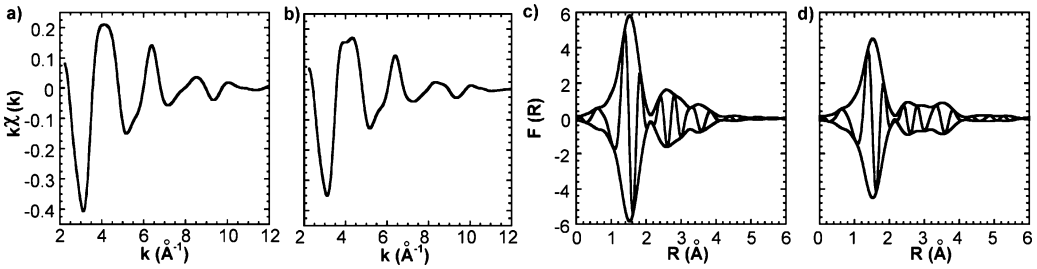

Figure 5. Experimental EXAFS spectra of **2a** and **3** (a and b, respectively) at room temperature and Fourier transformations (modulus and imaginary parts; c and d, respectively).

Table 4. Fit of the First-Shell Filtered EXAFS Spectrum of **2** Using a $N_2/O_2/N$ Model[a]

	n	σ (Å)	*R* (Å)	R_{XRDav} (Å)
N_{eq}	2	$9(1) \times 10^{-2}$	2.02(2)	2.01
O_{eq}	2	$6(1) \times 10^{-2}$	1.92(1)	1.95
N_{ax}	1	$9(4) \times 10^{-2}$	2.38(5)	2.46

[a] The number of atoms *n* in each shell is fixed. Debye−Waller factors σ and bond lengths *R* are fitted. The EXAFS distances are compared to the average crystallographic bond length R_{XRD}.

Trapping the Mononuclear Species (Reaction of 2 with Acetic Acid). Compound **2** was reacted with acetic acid in order to completely break the bis(μ-hydroxo) core of the dinuclear complex. The resulting EPR spectrum substantially increased in intensity, but was ill-defined and suggested the presence of several paramagnetic species. However, when the reaction was performed in the presence of a good guest such as acetamide, an intense signal (100% of the intensity expected for a mononuclear Cu(II) complex) characteristic of a single paramagnetic species (**3**)[18,21] was obtained (Figure 4). The EPR parameters of **3** ($A_{//} = 166 \times 10^{-4}$ cm^{-1}, $g_{//} = 2.285$, $g_{\perp} = 2.050$) are very close (although different, see Experimental Section) to those of compound **2b** in the presence of acetamide, and are clearly different from those of the parent dicationic complex.[22]

In UV−vis spectroscopy, the addition of aliquots of acetic acid to a THF solution containing **2** and acetamide led to the progressive extinction of the LMCT at 330 nm (Figure 5). An isobestic point at 314 nm attested to the concomitant formation of a single species. Beyond 1 equiv of added acetic acid per copper ion, the UV−vis spectrum did not further evolve, which suggests that the new complex **3** presents a Cu:ligand:metal stoichiometry of 1:1:1. The d−d band of **3** presents a maximum absorption of 707 nm ($\epsilon = 80$ M^{-1} cm^{-1}).

X-ray Absorption Measurements. Models for the Solid-State Structures of 2 and 3. To reach a better understanding of the structures of the monocationic mononuclear Cu(II) complexes, we undertook an EXAFS study on the isolated solid complexes **2** and **3**. As compound **2** in the solid state is composed of greater than 95% dinuclear species **2a**, we decided to model the EXAFS spectrum of **2** in the solid state on the basis of the X-ray structure depicted in Figure 2.

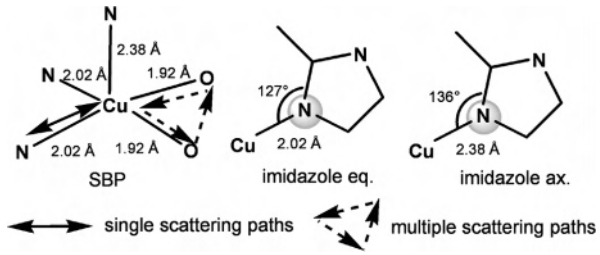

Figure 6. Models of fitted shells used for simulation of the complete EXAFS spectrum of **2**. The single paths of the circled atoms are not included in the imidazole groups, as they were already taken into account in the SBP group (step (i)).

Subsequently, we analyzed the EXAFS spectrum of **3**. Considering that **3** and **2b** have very similar structures (vide supra), this should provide valuable insights into the structure of mononuclear hydroxo complex **2b**, which could not be isolated. Acetato complex **3** was obtained by addition of 1 equiv of acetic acid to **2** in nitromethane in the presence of acetamide, followed by the evaporation of the solvent.

Each EXAFS spectrum is the average of four recordings at room temperature in the range 8920−9920 eV, including the copper K edge (∼8990 eV). The experimental EXAFS spectra of **2a** and **3** and their Fourier transformations (FT) are presented in Figure 5.

For both compounds, the FT presents a main peak related to the Cu(II) first coordination sphere (3N/2O) and secondary structures due to photoelectron scattering at longer distances. Such scattering contributions above 2 Å are typical of complexes containing imidazole ligands.[23] However, the scattering signal between 2 and 3 Å is more important for **2a** than for **3**. This reflects structural differences possibly related to the presence of Cu−Cu scattering in the dinuclear complex that is absent in the mononuclear complex.

EXAFS Modeling of 2. In the crystallographic structure of **2a**, both Cu(II) ions present similar environments and bond distances (Figure 2). To simplify the EXAFS model, we considered that both metal ions have identical environments (i.e., the complex was considered to be a perfect dimer). We proceeded in two steps with (i) refinement of the first

(21) Complex **3** could not be isolated as a pure compound; indeed, it is stable only in the presence of excess acetamide. Otherwise, it evolves toward multinuclear acetato−Cu(II) complexes.

(22) The EPR parameters (band X, 90 K) of the corresponding dicationic complex $[Cu(X_6Me_3Imme_3)(AcNH_2)(H_2O)](ClO_4)_2$ (Figure 1; R = Me, L = $AcNH_2$) are $g_{\perp} = 2.07$, $g_{//} = 2.31$, $A_{//} = 145 \times 10^{-4}$ cm^{-1}.

(23) (a) Zippel, F.; Ahlers, F.; Werner, R.; Haase, W.; Nolting, H.-F.; Krebs, B. *Inorg. Chem.* **1996**, *35*, 3409−3419. (b) Pascaly, M.; Duda, M.; Rompel, A.; Sift, B. H.; Meyer-Klaucke, W.; Krebs, B. *Inorg. Chim. Acta* **1999**, *291*, 289−299. (c) Sabatucci, A.; Ascone, I.; Beltramini, M.; Muro, D.; Salvato, B. *J. Biol. Inorg. Chem.* **2002**, *7*, 120−128. (d) Hasnain, S. S.; Diakun, G. P.; Knowles, P. F.; Binsted, N.; Garner, C. D.; Blackburn, N. J. *Biochem. J.* **1984**, *221*, 545−548. (e) Pettifer, R. F.; Foulis, D. F.; Hermes, C. *J. Physiol.* **1986**, *12* (4), C8-545−C8-550.

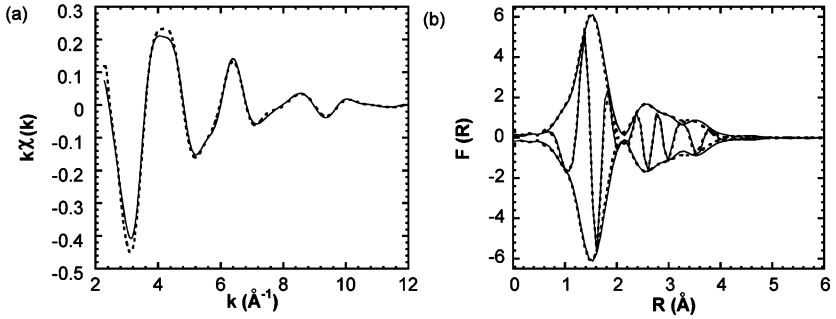

Figure 7. Comparison between experimental and simulated spectra of **2a**: (a) EXAFS spectra; (b) Fourier transformation modules and imaginary parts. Plain lines: experimental spectra. Dotted lines: simulated spectra.

Table 5. Fit of the Complete EXAFS Spectrum of **2** Using a Four-Shell Model[a]

shell modeled	*n*	σ (Å)	ΔR (Å)	φ_i (deg)	XRD angles (deg)
SPB	1	0.075(4)	−0.02(1)		
Cu···Cu	1	0.09(1)	−0.03(4)		
eq. imidazole	2	0.13(6)	0.03(5)	127	$\varphi_{1av} = 132$
ax. imidazole	1	0.11(15)	0.1(2)	136	$\varphi_2 = 139$

[a] The number of atoms *n* in each shell is fixed. Debye−Waller factors σ and effective distance shifts ΔR are fitted. The angles are compared to the average crystallographic angles. There are 24 independent points and 8 fitted parameters. φ_i angles are defined in Figure 6.

Table 6. Fit of the First-Shell Filtered EXAFS Spectrum of **3** Using a N_3/O/N Model[a]

	n	σ (Å)	*R* (Å)
N/O	3	$11(2) \times 10^{-2}$	2.01(2)
N/O	1	$5(2) \times 10^{-2}$	1.92(2)
N/O	1	$8(3) \times 10^{-2}$	2.38(3)

[a] The number of atoms *n* in each shell was fixed. Debye−Waller factors σ and bond lengths *R* were fitted. The quality factor of this fit is 4.48.

coordination sphere and (ii) refinement of the complete spectrum up to 4 Å.

(i) The first-shell filtered spectrum was simulated by using three distinct components (2 O_{eq}, 2 N_{eq}, and 1 N_{ax}), whose phases and amplitudes were calculated with FEFF7.[24] The distances and Debye−Waller factors of each shell, as well as a global ΔE parameter, were refined using the EXAFS analysis package EXAFS pour le Mac.[25] The distances obtained are in good agreement with the crystallographic data (Table 4). Nevertheless, the EXAFS bond length of the axial ligand appeared to be slightly underestimated. The −1.58 eV value for the extra parameter ΔE brought the edge energy to 8987.4 eV. This value was then kept for all fits for both compounds. The quality factor of the fit was excellent (0.72).

(ii) The complete EXAFS spectrum of **2a** could be modeled ab initio up to 4 Å from the crystallographic data using FEFF7. An analysis of the scattering path contributions

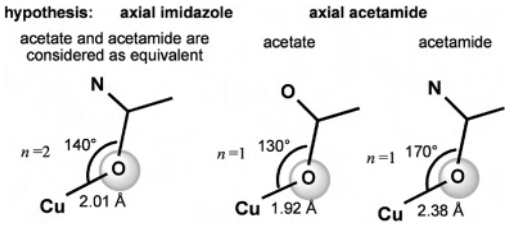

Figure 8. Models of fitted shells used for simulation of the acetamide and the acetate in both hypotheses. The single paths of the circled atoms are not included in the shell.

showed it was possible to limit the refinement of the copper neighborhood to four groups of atoms (Figure 6): (1) the square-based pyramid (SBP), (2) two equivalent equatorial imidazoles, (3) the axial imidazole, and (4) the second copper. It was thus possible to refine the complete model using average parameters for these groups. The global phase and amplitude of each group were calculated from the partial theoretical EXAFS signals calculated by FEFF7. For each group, we refined an effective distance shift and Debye−Waller factor. For the two imidazole groups, we also refined an orientation angle as described in Figure 6. The parameters of the best simulation are presented in Table 5. The quality factor of the fit is excellent (0.22). The refined distance-shift values are close to zero, most of them within the error bars. The refined imidazole angles are also in good agreement with the crystal structure.

Figure 7 presents the comparison between experimental and refined FEFF-simulated EXAFS spectra of compound **2**. The four-shell model detailed above correctly fits the complete EXAFS spectrum. Importantly, it must be emphasized that such a good model, with a quality factor of 0.22 for dinuclear complex **2**, cannot be obtained without the presence of the Cu−Cu contribution. Indeed, the best-fit quality factor of a Cu−Cu free model was 0.31. According to the F-test,[26] adding the Cu−Cu contribution to the model improved it with a 77% level of probability.

EXAFS Modeling of 3. The EXAFS spectrum of mononuclear complex **3** was modeled with a similar approach. The main difference between the molecular structures of compounds **2a** and **3** is that the hydroxo-bridging ligands are replaced by one acetato and one acetamido *O*-ligand. In

(24) (a) Rehr, J. J.; Zabinsky, S. I.; Albers, R. C. *Phys. Rev. Lett.* **1992**, *69*, 3397−3400. (b) Rehr, J. J. *Jpn. J. Appl. Phys.* **1993**, *32*, 8. (c) Rehr, J. J.; Mustre de Leon, J.; Zabinsky, S. I.; Albers, R. C. *J. Am. Chem. Soc.* **1991**, *113*, 5135−5540. (d) Mustre de Leon, J.; Rehr, J. J.; Zabinsky, S. I.; Albers, R. C. *Phys. Rev. B* **1991**, *44*, 4146−4156. (e) Rehr, J. J.; Albers, R. C. *Phys. Rev. B* **1990**, *41*, 8139−8140.

(25) (a) Michalowicz, A. *Logiciels pour la Chimie*; Société Française de Chimie: Paris, 1991; p 102. (b) Michalowicz, A. *J. Phys. IV* **1997**, *7*, 235−236. (c) Catalog of EXAFS programs of the International XAFS Society: http://ixs.csrri.edu/IXS/catalog/XAFS_Programs.

(26) (a) Joyner, R. W.; Martin, K. J.; Meehan, P. J. *J. Phys. C* **1987**, *20*, 4005−4012. (b) Provost, K.; Champloy, F.; Michalowicz, A. *J. Synchrotron Radiat.* **2001**, *8*, 1109−1112.

Table 7. Fit of the Complete EXAFS Spectrum of **3** for Both Hypotheses[a]

axial imidazole hypothesis[b]				axial acetamide hypothesis[b]			
shell modeled	*n*	σ (Å)	ΔR (Å)	shell modeled	*n*	σ (Å)	ΔR (Å)
SBP	1	$9.5(2) \times 10^{-2}$	−0.03(1)	SBP	1	$9.5(2) \times 10^{-2}$	−0.03(1)
eq. imidazole	2	$8(1) \times 10^{-2}$	−0.07(1)	imidazole eq	3	$9.9(6) \times 10^{-2}$	−0.04(1)
acetamide/acetate	2	$7(1) \times 10^{-2}$	0.00(1)	acetate	1	$3(1) \times 10^{-2}$	0.13(1)
ax. imidazole	1	$10(3) \times 10^{-2}$	−0.09(4)	acetamide ax	1	$11(1) \times 10^{-2}$	0.07(1)

[a] The number of atoms *n* in each shell is fixed. Debye−Waller factors σ and effective distance shifts ΔR were fitted. There are 31 independent points and 8 fitted parameters. [b] $\Delta\chi^2_\nu$, the quality factor of the simulation, is equal to 0.72 for the axial imidazole hypothesis and 1.60 for the axial acetemide hypothesis.

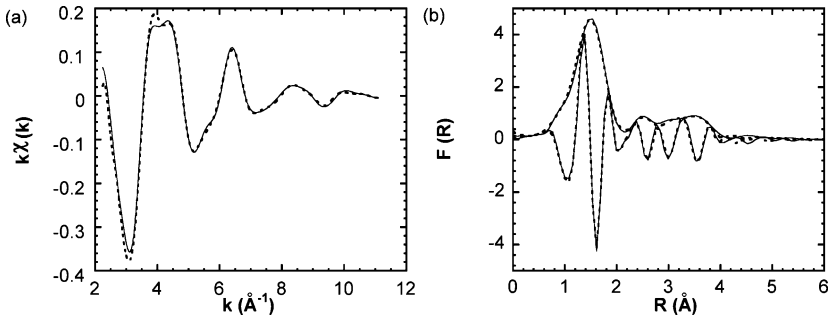

Figure 9. Comparison between experimental and simulated spectra of **3**: (a) EXAFS spectra; (b) Fourier transformation modules and imaginary parts.

such a square planar coordination, two structural possibilities must be considered: the axial ligand can be one imidazolyl arm (as is the case in the dicationic cupric complex),[8] or it can be one *O*-donor (acetamide or acetate).

The best fit of the filtered spectrum corresponding to the first coordination sphere gave three distances: three atoms at 2.01 Å, one at 1.92 Å, and one at 2.38 Å (Table 6). Obviously, the longest distance corresponds to the axial ligand, and the two others correspond to the equatorial positions. However, it is impossible to distinguish between nitrogen and oxygen single-scattering EXAFS signals. Thus, at this step, both structural hypotheses are still feasible.

The complete EXAFS spectrum of **3** was then modeled with an approach similar to that followed for **2**. The SBP and imidazoles were modeled in the same way as for **2**. After fitting φ_1 and φ_2, these angles were fixed to 130 and 133°, respectively. The two hydroxo bridges were replaced by two new groups, acetato and acetamido, that cannot be distinguished. As for the imidazole groups, an orientation angle was refined. The angle values giving the best simulations are reported in Figure 8. The parameters of the best simulation for each hypothesis are presented in Table 7.

In both models, the effective distance shifts are reasonably close to zero. However, the quality factor of the first model (axial imidazole) is significantly better than in the case of the axial acetamide hypothesis: the F-test comparison between the two models gives a probability level of 97% in favor of model (i). The good quality of this model is shown in Figure 9. It was obtained without any contribution of a Cu−Cu signal, which validates the mononuclear assumption made for **3**.

On the basis of these results, we propose that in complex **3**, the axial ligand is one of the imidazole arms, whereas the anionic ligand and acetamide are in a trans position, as shown in Scheme 1. This geometry is similar to that observed in the crystallographic structures of the parent dicationic complexes.[8]

Conclusion

The mononuclear Cu(II) aqua complex based on a calix[6]tris(imidazole) ligand reacts with a base to provide the corresponding hydroxo complex **2**. The latter has been characterized in the solid state by X-ray diffraction and absorption spectroscopies. It presents a dinuclear structure with a classical μ-$(OH)_2Cu_2$ core. Three imidazole arms wrap each Cu(II) ion, one being deeply included in the heart of the hydrophobic cavity, the two others coming from two different calixarene units, which further stabilizes the edifice. In solution, the presence of a mononuclear species was detected. An equilibrium between both species was observed, as the proportion of species **2b** slightly increased upon dilution or upon the addition of a small organic guest ligand. The latter is believed to displace the equilibrium by ejecting the endo-coordinated imidazole arm, thereby destabilizing the dinuclear edifice. Whereas the host−guest interaction was not strong enough to fully displace the equilibrium in favor of the mononuclear hydroxo species **2b**, it allowed for the stabilization of the acetato derivative. Indeed, in the presence of a good guest ligand (acetamide), the mononuclear hydroxo species could be trapped by acetic acid, leading to the quantitative formation of a novel monocationic complex **3**. The UV−vis and EPR spectra were in agreement with a mononuclear core resembling the parent dicationic aqua complex, with an acetato ligand in place of the water molecule. EXAFS studies first performed on complex **2** in the solid state allowed very nice modeling of the complex, clearly highlighting the dinuclear core and the five-coordinate environment provided by the imidazoles. The subsequent analysis of **3** by EXAFS led to a highly reliable model that fully supported the proposed structures.

Taken together, these results emphasize some important characteristics of the calix[6]arene-based ligands. First, their high flexibility allows them to accommodate various geometries and various nuclearities, from mono-[8] to di-, tri-[27] and

tetranuclear.[16] The associated cavity behaves as a remarkable host for organic neutral moieties, as it can include small neutral organic ligands but also undergo self-inclusion of an imidazole arm. This last process opens a second coordination site oriented to the outside, which enables the building of a double-bridging unit. One of the keys to this last process seems to be the reluctance of the calixarene core to bind anionic species (OH^-, AcO^-), as has been previously observed in many instances.[28,29] This is probably due to both the proximate oxygen atoms of the phenolic units and the π-basic character of the calixarene cavity. Hence, this work nicely illustrates the decisive role of both the second coordination sphere and the supramolecular host−guest interactions for the stabilization of a metal complex.

Acknowledgment. The authors gratefully acknowledge support from the CNRS and the Ministère de la Recherche (G.I.), and thank Dr. O. Sénèque (UMR 8601) for his help in growing single crystals of **2**.

Supporting Information Available: Crystallographic data in CIF format. This material is available free of charge via the Internet at http://pubs.acs.org.

IC0511322

(27) Izzet, G.; Akdas, H.; Hucher, N.; Giorgi, M.; Prangé, T.; Reinaud, O. Submitted.
(28) Darbost, U.; Zeng, X.; Rager, M.-N.; Giorgi, M.; Jabin, I.; Reinaud, O. *Eur. J. Inorg. Chem.* **2004**, 4371−4374.
(29) Izzet, G.; Douziech, B.; Prangé, T.; Tomas, A.; Jabin, I.; Le Mest, Y.; Reinaud, O. *Proc. Natl. Acad. Sci. U.S.A.* **2005**, *102*, 6831−6836.